Break-up induced by the collapse of laser-generated cavitation bubbles in a liquid jet

Jiayi Zhou*, Mats Andersson
Department of Mechanics and Maritime Sciences, Chalmers University of Technology, Sweden

Abstract

In this paper, the effect of artificially introduced cavitation bubble collapse on jet break-up was studied. Laser-induced cavitation bubbles were introduced into the jet at the exit of a scaled-up nozzle. Shadow images of the jet or spray were recorded by a high-speed video camera. The break-ups, which were induced by bubble collapse, were measured, compared and analyzed under different injection pressures and bubble generating positions. The study shows how the collapsing laser-induced cavitation bubbles outside of the nozzle affect jet break-up. The break-ups were categorized into two characteristic types. The distance of the laser focus to the center axis of the nozzle was found to be the main factor that determined the type of break-up.

Keywords: Spray, atomization, cavitation, break-up

Introduction

Since Bergwerk [1] found that both cavitating and non-cavitating flow in diesel nozzles may occur under different conditions in the 1950s, formation and characteristics of the cavitation inside the fuel injector nozzle and how cavitation affects the atomization of fuel outside the nozzle have been studied extensively. Especially when the climate change caused by greenhouse gas and other pollutant emissions is becoming a severe problem and governments of various countries and organizations are implementing stricter legislations on the emissions from liquid-fueled transportation, more attention has been paid to research of fuel injection system of engines. Cavitation which originates inside the nozzle is believed to be an important mechanism causing atomization in the sprays [2]. To investigate the cavitation inside the nozzle and its effect on fuel atomization, numerous optical diagnostic methods have been applied to observe and detect the flow inside and outside the nozzle. Usually, internal flow is visualized by using transparent nozzles and shadowgraph imaging with high speed cameras, and its velocity is measured by particle image velocimetry (PIV) [3], [4]. The velocity and droplet size distribution of the spray outside the nozzle can be measured by Phase Doppler Anemometry (PDA) [5], and the whole view and outskirt behavior like spray cone angle can be obtained by shadowgraph imaging. Compared to the ones inside the nozzle, cavitation bubbles outside the nozzle are more difficult to observe because they are surrounded by droplets and liquid phase jet. To solve this problem, a special near-nozzle field visualization of cavitation bubbles has been carried out by injecting the fuel in a liquid environment of a pressurized fuel chamber [6].

It is widely proved that collapse of cavitation bubbles enhances atomization [7], [8], [9], [10]. However, it is not easy to study the influence of the collapse on jet break-up, separately. For experiments, one always needs to induce cavitation bubbles at proper conditions and observe the whole process from cavitation formation inside the nozzle to jet break-up outside the nozzle. For simulations, it is necessary to calculate the multiphase flow inside and outside the nozzle. In this study, in order to concentrate on the effect of bubble collapse on jet break-up without dealing with cavitation bubble formation and distribution inside the nozzle, cavitation bubbles were artificially introduced in the near nozzle region of a jet by focusing laser light into the jet. The laser-induced cavitation bubble technique has been widely used in researches of cavitation erosion, film-free laser forward printing, and so on [11], [12]. In this study, this non-invasive technique was chosen because, in this way, the jet would not be disturbed by additional experimental elements, for example, the electric nodes which are used to generate bubbles in some investigations [13], [14].

In this study, an experimental setup was established to investigate cavitation bubble collapse-induced jet break-up. The light from a pulsed laser was focused into the jet at the exit of a scaled-up nozzle orifice to generate a cavitation bubble in the primary break-up region. Shadow images of the jet or spray were recorded by a high-speed video camera which was positioned in the perpendicular direction to the laser beam. Shape of the fragments, which were broken up from the jet by bubble collapse, and development rate of jet or spray were measured, compared and analyzed under different in-nozzle flow conditions and bubble generating positions.

Experimental Methods

The experimental setup consisted of three main parts which were shadowgraph imaging, laser beam focusing, and liquid injection. A schematic of the setup is shown in Figure 1. The shadowgraph part had a plasma lamp acting as the light source. The diverged light source was collimated by lens L1. The collimated light passed through the near nozzle orifice region to illuminate the primary break-up region of the spray. The high-speed

video camera located at the other side of the nozzle captured shadowgraph videos of the spray. A filter was put in front of the camera lens to block the scattered laser light. The laser beam focusing part contained a Nd: YAG laser which could provide ns-laser pulses. The power of the laser beam was reduced by the attenuator which was composed of a half wave plate and a Glan-laser prism. The energy was adjusted by rotating the half wave plate with a micrometer screw for fine tuning. The energy-reduced laser beam was expanded by the concave lens L2 and the convex lens L3, and then focused under the nozzle by focal lens L4. The aim of expanding the laser beam before focusing it into the jet was providing a larger focusing angle which would generate a compact plasma, hence, a spherical bubble [11]. The lens L4 mounted on a micrometer translation stage could be moved along the laser beam direction. In this way, the horizontal position of the beam focus could be varied by moving lens L4. The liquid injection part [15] had an acrylic nozzle of which inner diameter was 6 mm. The inlet of this nozzle was round, so no cavitation was introduced into the nozzle. The nozzle was connected to an accumulator which was held by two vertically mounted electric motor-driven translation stages. The relative vertical position of the laser beam focus to the nozzle orifice could be varied by adjusting the height of the accumulator together with the nozzle via these two translation stages. The liquid inside the nozzle and accumulator was driven by compressed nitrogen. The high-pressure gas pushed the liquid inside the accumulator and forced the liquid to be ejected through the nozzle. The injection direction was same as gravity direction. The injection pressure was adjusted by a pressure regulator connected to the nitrogen bottle.

In the experiment, the Nd: YAG laser and the high-speed video camera were synchronized by delay generators. The laser was triggered by a delay generator externally. The pulse energy, wavelength and frequency of the laser were 5mJ, 532 nm and 10 Hz respectively. The frame synchronization signal of the camera was externally provided by the delay generators. The sample rate was 41056 fps. The camera was controlled to start to capture before each laser pulse with a time gap of 297 μs, and pause after 4.9 ms which was the length of each video fragment. The distance between the laser focus and the axis of nozzle varied from 1 mm to 3.5 mm with an interval of 0.5 mm. The liquid used in the experiment was deionized water. The injection pressure was set to be from 1.1 bar to 6 bar over atmosphere with an interval around 0.5 bar. The ambient pressure was atmosphere.

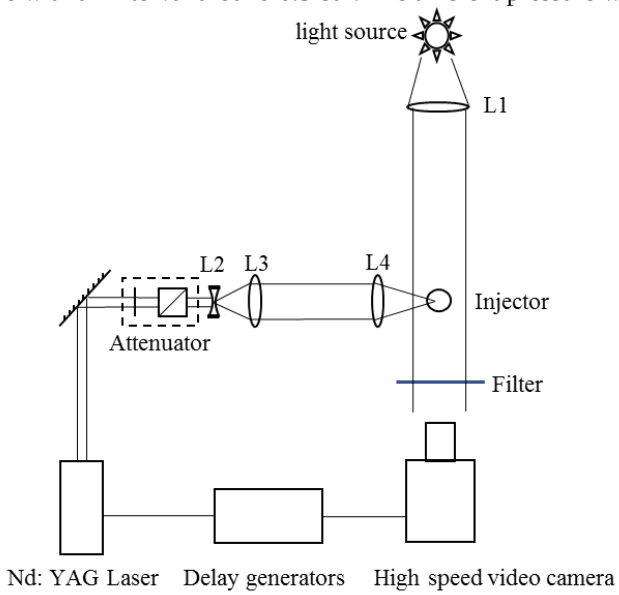

Figure 1 Schematic of the experiment setup.

Results and Discussion

The shapes of break-ups induced by collapse of cavitation bubble varied a lot in different experiment conditions such as different injection pressures and distances between the laser focus and the axis of the nozzle. Even for the same condition, the break-ups could be different from pulse to pulse. However, regularities were found after some qualitative and quantitative analysis. In the following results, the distance between the laser focus and the axis of the nozzle and injection pressure are denoted as ‘d’ and ‘P’ respectively.

Based on the shapes, the break-ups can be divided into two types. One is called small break-up shown in Figure 2 (a), the other is massive break-up shown in Figure 2 (b). Their photos are chosen from two different video sequences which were taken in two experiment conditions; for Figure 2 (a), d=1.5 mm, and P=1.6 bar, while for Figure 2 (b), d=2.5 mm, P=3.6 bar. The time under each photo is counted from the moment of the laser pulse emission. For the small break-up, there is only one main spike ejected from the jet. The tip of the spike separates into tiny droplets quickly, and is followed by a ligament which breaks up later as well. During the recording

period, there are quite few break-ups besides the one induced by the collapse of the artificially introduced cavitation bubble. For the massive break-up shown in Figure 2 (b), multiple ejected spikes are breaking up from the jet at 0.1 ms. Then at 0.5 ms, a large fragment is coming out of the jet. The fragment is separating into more ligaments at 1 ms and 1.5 ms. At last, these ligaments are breaking into droplets as is shown in the photo of 2 ms. During this recording period, due to the increased injection pressure, there are more break-ups beside the one induced artificially. However, the cavitation bubble induced break-up comes earlier and spreads wider in the radial direction of jet.

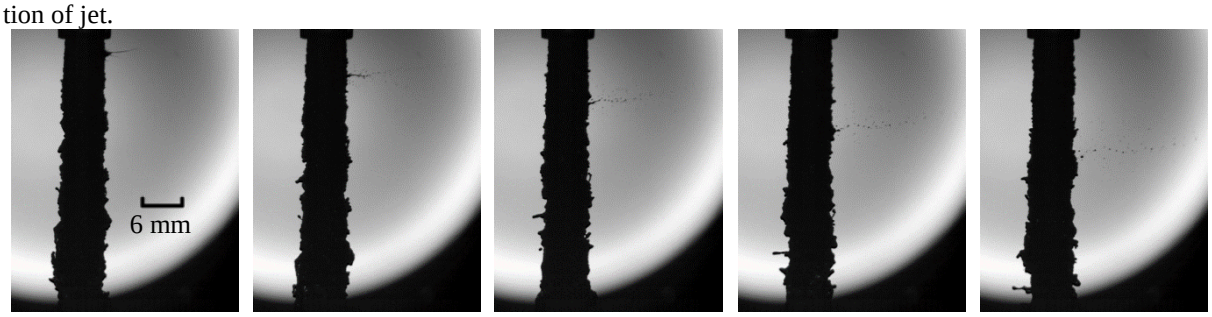

(a) small break-up

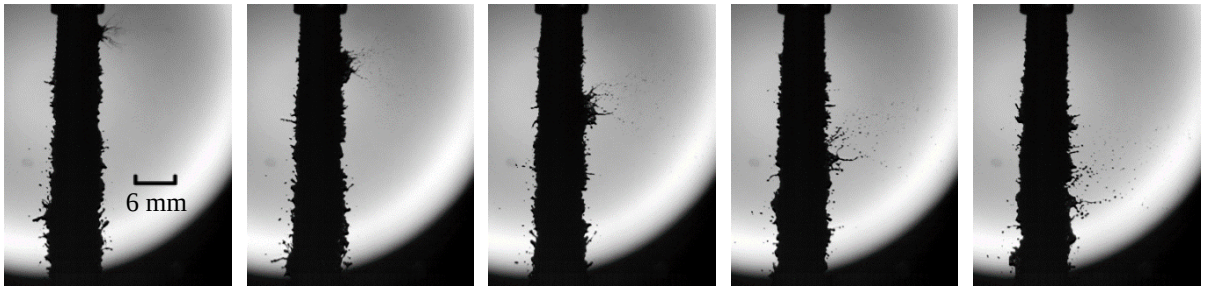

(b) massive break-up

Figure 2 Small and massive break-ups at different conditions. (a) d=1.5 mm, P=1.6 bar. (b) d=2.5 mm, P=3.6 bar. The times indicated under each image is the time after the laser pulse.

The break-ups shown in Figure 2 are examples of the two typical types at the two experiment conditions. However, it is worth to mention that these two types are not specific for these two conditions. The small break-ups also came out at higher injection pressure and vice versa. To figure out which factor affects the break-up type most, a quantitative analysis on projected 2-dimentional (2D) spray area change rate was performed. As shown in Figure 3, a rectangular region, whose position is fixed in every photo, is binarized. The binarization keeps the main body of the jet and the large break-up structures like large droplets, the ejected spikes, and fragments shown in Figure 2, while it discards the droplets that are too small or move too far away from the jet. The normalized 2D spray area is the ratio of the number of the pixels that are 1 to the amount of all pixels in the selected region. In Figure 4, the change rate is the difference of the normalized spray area with respect to time. Figure 4 shows the results at the conditions of d=1 mm to d= 3.5 mm when the injection pressure is 1.1 bar. These are the averaged results from 15 repetitive experiments except the d=1 mm one which is the average of 2 samples, since most events with d=1 mm did not produce clearly identifiable break-ups. For most cases, there is an obvious peak right after 0 ms when the laser pulse arrives. The rapid increase of the area change rate represents the fast development of the bubble collapse induced break-up right after the laser pulse. Figure 4 (b) shows the partial enlarged diagram of Figure 4 (a). The highest peak is found at d=2.5 mm. For most cases except d=2.5 mm, the area change rate decreases rapidly to around zero, which means the relatively large break-up structure only exists for a short time after the laser pulse and separates into tiny droplets quickly. The small break-up shown in Figure 2 (a) fits this result. For d=2.5 mm, there is an extended decreasing slope crossing the zero change rate level at around 2 to 2.5 ms. This extended slope shows that the large break-up structures continue developing for longer time before they turn into tiny droplets. The negative part of the change rate is caused by big fragments turning into tiny droplets and moving out of the selected region. The massive break-up shown in Figure 2 (b) fits the result of d=2.5 mm.

Figure 4 (b) shows the d-dependent peak spray area change rates. The exact reason of this result needs more work in the future, but a preliminary analysis was made based on research on liquid ejections induced by cavitation bubble collapse beneath free surfaces [12], [13], [14], [15], [16]. The velocity of the ejection increases as the

bubble size gets larger and decreases as the distance from the bubble to the surface gets longer. In our cases, when d was smaller, the distance from the bubble to the surface of jet became longer. Thus, the trend of increasing area change rate as d increased from 1 to 2.5 mm, is consistent with a higher ejection velocity with a bubble location closer to the surface. At the same time, the laser light energy going into bubble formation might have been reduced as the laser beam focus moving farther from the jet surface which was roughly cylindrical and unsmooth, making the focus less sharp. This effect would further contribute to a smaller area change rate for smaller d. While for d=3 mm and 3.5 mm, where the bubbles collapsed almost on the jet surface, possibly even before it had time to grow to its maximum size, the jet was torn into droplets directly without the formation of spike, ligament or fragment shown in Figure 2. Some of these droplets were too small and discarded by the binarization, so the spray area change rates became smaller. .

Similar results were found for higher injection pressures. Different break-up types were mostly determined by the distance of the laser focus to the axis of the nozzle. The main differences of the results at higher injection pressures from the one shown in Figure 4 were that, as the injection pressure went higher, the peaks right after the laser pulse became smaller and the spray area change rate was more fluctuating. In Figure 5, when the injection pressure is 5 bar, the peaks are not so obvious compared to the fluctuations. There were two main reasons for the difference. One was that there were more spontaneous break-ups due to higher injection pressure, so the proportion of the bubble collapse induced break-ups to the total break-up events was smaller. The other one was that the amount of laser light energy going into bubble formation was likely reduced due to the unsmooth jet surface as the injection pressure became higher.

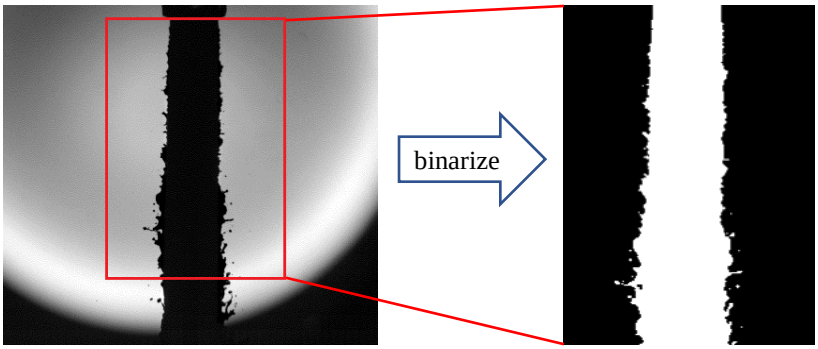

Figure 3 Selected and binarized region for calculating spray area.

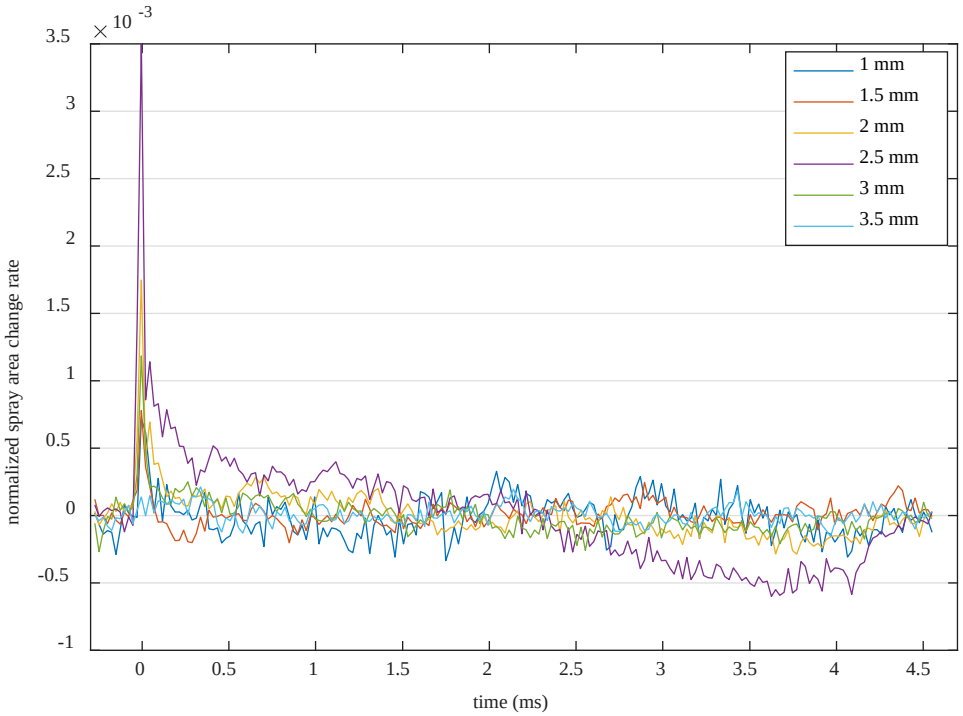

(a)

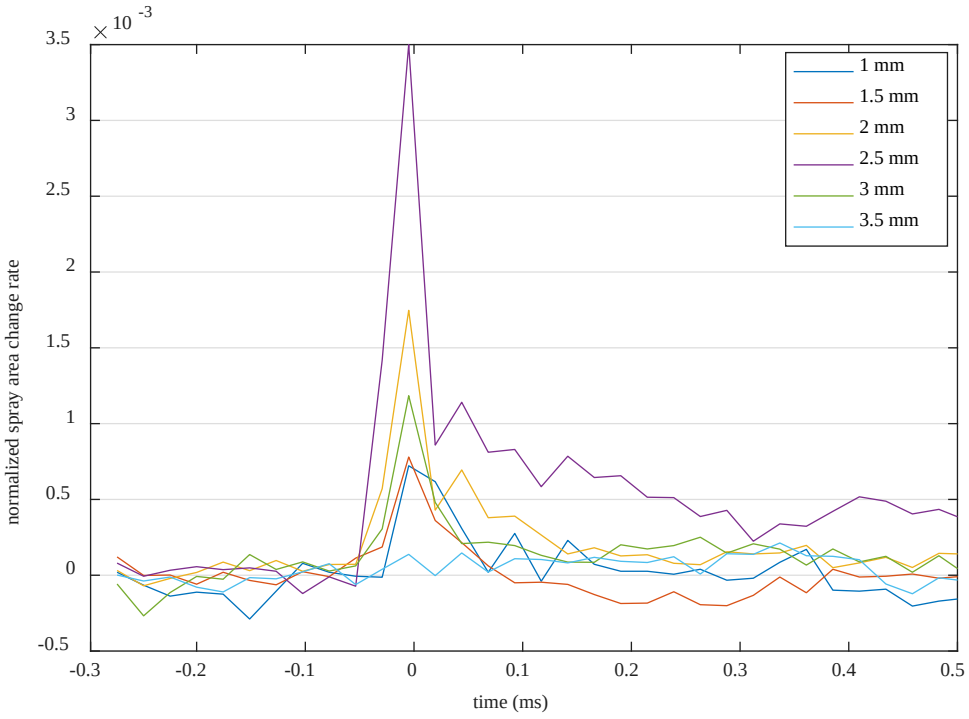

(b)

Figure 4 Normalized spray area change rate for various d when the injection pressure was 1.1 bar.

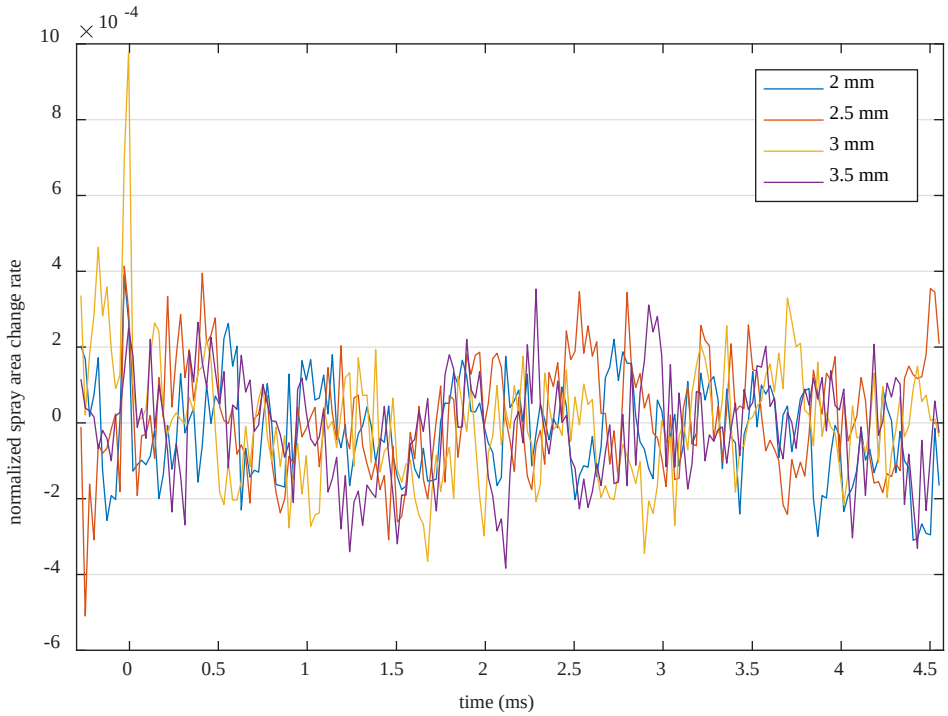

Figure 5 Normalized spray area change rate for various d when the injection pressure was 5 bar.

Summary and Conclusions

In this study, an experimental setup was established to introduce laser-induced cavitation bubbles into the primary break-up region of spray. Shadow images of the bubble collapse-induced break-up events were recorded by a high-speed video camera. Break-ups at different experimental conditions were analyzed, compared, and then categorized into two characteristic types. The distance of the laser focus to the center axis of the nozzle was found to be the main factor that determined the type of break-up.

In the current study, there are still some uncertainties that inspire future work. The laser-induced cavitation bubbles were not visible in the shadow images, so it was difficult to know the relationship between the bubbles and break-ups directly. For example, the mechanism of how the bubble induced the break-up was unclear. The relationship between the characteristics of bubble and the break-up was unclear as well. This paper only presented the results by using deionized water. To get results at more conditions, other liquids with different viscosities and surface tensions will be used in a future study.

Acknowledgements

Financial support was obtained through the project “HAoS - Holistic Approach of Spray Injection through a Generalized Multi-Phase Framework”, a Marie-Skłodowska-Curie Innovative Training Network, project ID 675676-HAoS-H2020-MSCA-ITN-2015.

References

[1] Bergwerk, W., *Proceedings of the Institution of Mechanical Engineers* 173: 655-660 (1959).
[2] Soteriou, C., Andrews, R., and Smith M., *SAE International*, 1995.
[3] Hayashi, T., Suzuki, M., and Ikemoto, M., *12th Triennial International Conference on Liquid Atomization and Spray Systems*, 2012.
[4] Hult, J., Simmank, P., Matlok, S., Mayer, S., Falgout, Z., and Linne, M., *Experiments in Fluids* 57: 49 (2016).
[5] Mitroglou, N., Gavaises, M., Nouri, J.M., and Arcoumanis, C., in: Cossali, G.E., Tonini, S. (Eds.) *Droplet Impact Phenomena and Spray Investigations Workshop 2011, Dip. Ingegneria industriale*, Università degli studi di Bergamo, Bergamo, Italy, 2011.
[6] Payri, R., Salvador, F.J., Gimeno, J., and de la Morena, J., *International Journal of Heat and Fluid Flow* 30: 768-777 (2009).
[7] Payri, R., García, J.M., Salvador, F.J., and Gimeno, J., *Fuel* 84: 551-561 (2005).
[8] Sou, A., Hosokawa, S., and Tomiyama, A., *International Journal of Heat and Mass Transfer* 50: 3575-3582 (2007).
[9] Suh, H.K., Lee, C.S., *International Journal of Heat and Fluid Flow* 29: 1001-1009 (2008).

[10] Örley, F., Trummler, T., Hickel, S., Mihatsch, M.S., Schmidt, S.J., and Adams, N.A., *Physics of Fluids* 27: 086101 (2015).
[11] Brujan, E.-A., Nahen, K., Schmidt, P., and Vogel, A., *Journal of Fluid Mechanics* 433: 251-281 (2001).
[12] Patrascioiu, A., Fernández-Pradas, J.M., Morenza, J.L., and Serra, P., *Applied Surface Science* 302: 303-308 (2014).
[13] Obreschkow, D., Kobel, P., Dorsaz, N., de Bosset, A., Nicollier, C., and Farhat, M., *Physical Review Letters* 97: 094502 (2006).
[14] Ji, C., Li, B., Zou, J., and Yang, H., *Experimental Thermal and Fluid Science* 81: 76-83 (2017).
[15] Sedarsky, D., Falgout, Z., Rahm, M., and Linne, M., *27th Annual Conference on Liquid Atomization and Spray Systems, ILASS Americas*, Raleigh, NC, USA, 2015.
[16] Pearson, A., Cox, E., Blake, J.R., and Otto, S.R., *Engineering Analysis with Boundary Elements* 28: 295-313 (2004).